Thermal Science and Engineering Progress 19 (2020) 100583

Contents lists available at ScienceDirect

Thermal Science and Engineering Progress

journal homepage: www.elsevier.com/locate/tsep

Exergy and parametric analysis of freeze desalination with reversed vapor compression cycle

M.A. Abd Elrahman[b], Saber Abdo[a,*], Eslam Hussein[b], Ahmed A. Altohamy[b], Ahmed A.A. Attia[b]

[a] Mechanical Engineering Department, University of Bristol, UK
[b] Combustion and Energy Technology Lab, Mechanical Engineering Department, Shoubra Faculty of Engineering, Benha University, Egypt

ARTICLE INFO

Keywords:
Freeze desalination
Salinity
Ice ratio
freshwater productivity. Exergy

ABSTRACT

Freezing desalination is one of the recent technologies that tries to contribute in water shortage problems. The idea of desalination by freezing is quite new and still needs more deep investigation for better understanding and proposing new enhancements in the system's technology. This paper aims to present exergy and parametric analysis for different operational parameters of a small-scale desalination by freezing unit working on a reversed vapor compression cycle. Operating parameters including freezing ratio, temperature and salt concentration are investigated. These parameters variations are critical to determine the working design parameters effects on the overall cycle performance. Salinity range from 5000 to 45000 ppm was tested using a heat pump of a C.O.P range from 3.8 to 8.2. Results showed that the energy consumption for this system range was 14.5 and 68.7, kWh per meter cube water production at 5000 and 45000 ppm, respectively. Exergy analysis showed that recovering larger quantities of the expelled brine is more efficient and useful due to more contributions in increasing the energy efficiency of the operating cycle. The proposed system proved to give higher thermal efficiency compared to alternative desalination systems such as reverse osmosis with membranes or flash systems. The system recorded a high thermal efficiency of 44% at 25 °C and 50% icing ratio. The output results from the system analysis given in this paper could significantly help to implement an actual optimized desalination system working on a reversed vapor compression cycle.

1. Introduction

The water demand is increasing in both industrial and domestic sections and at some point, it will be higher than the agriculture demand as reported in[1],[2], [3] and [4]. Desalination is one of the most important solutions for water supply as it is a reliable technology that was improved over decades to overcome fresh-water shortage by processing seawater in different ways and convert it into freshwater. In 2017, water desalination plants reached very high capacities of 99.8 million m3/day [5] and [6].

As reported in [7], suitable conditions and disposal location availability are the most limiting key factors while building a seawater desalination plant due to the generated high-salinity brine. Freezing based desalination is categorized as one of the phases change process desalination techniques. Freezing Desalination (FD) has been improved and tested in different ways because of its advantages over both membrane and thermal based desalination techniques. In a related study, Brenda Kalista, et al [8] highlighted the main concepts behind FD process by providing a deep explanation for the process itself and their different applications and how to integrate it with other desalination technologies. Freezing desalination process mainly depends on a seawater phase change process from the liquid phase to the solid phase "ice". In theory, most ice crystals contain pure water [9] and [10]. Hence, fresh water can be extracted from the formed ice after the complete freezing process while the salt is disposed as a high concentration brine.

The FD processes can be classified into direct and indirect processes [11]. In the direct freezing process, the heat is absorbed from the saline water while the refrigerant enters the crystallizer. Simultaneously, saline-water temperature decreases, and nucleation starts to occur. This process offers high economic efficiency, large surface area, and increased heat transfer coefficient because of the direct contact [12].

For the indirect freezing process, a crystalliser wall separates the refrigerant from the saline water. This gives the indirect method an advantage over the direct freezing method which is the product water is a refrigerant-free product. Worth mentioning that, the indirect method induces nucleation and ice crystals growth complexity that increases

* Corresponding author.
E-mail addresses: Mohamed.abdelrahman@feng.bu.edu.eg (M.A. Abd Elrahman), Saber.abdo@bristol.ac.uk (S. Abdo), Islam.hussein@feng.bu.edu.eg (E. Hussein), Ahmed.soliman@feng.bu.edu.eg (A.A. Altohamy), Ahmed.attia@feng.bu.edu.eg (A.A.A. Attia).

https://doi.org/10.1016/j.tsep.2020.100583
Received 14 July 2019; Received in revised form 10 May 2020; Accepted 25 May 2020

Nomenclature

CR	Concentration Ratio
C.O.P	Coefficient of Performance
cond	Condenser
comp	Compressor
C.V	Control Volume
ev	Evaporator
exp	Expansion device
Ex	Exergy kJ/kg
EXD	Exergy destructive kj/kg
gen	Generation
HP	Horse Power
L.H.F	Latent heat of freezing J/kg.
p.p.m	Particle per million
b	Brine.
C_p	Specific heat J/kg K.
d	Distillate
E	Specific Energy consumed J/kg
g	Gravitational acceleration m/s^2
f	Feed
f	Refrigerant
h	Specific Enthalpy J/kg
i	Input
L	Logarithmic array
M	Mass Kg
$\dot{m}$	Mass flow rate kg/s
n	Total number of trials
N_T	the minimum number of trials
N_P	the number of parameters
N_L	The number of levels of each parameter.
o	Output
P	Pressure
P_o	Atmospheric pressure
q_L	Cooling effect Joule
Q_{cv}	Control volume heat rate J/s
q_c	Reject heat
R	Ice Ratio
S	Salinity percentage %
s	Specific Entropy J/kgk
S/N	Single to noise ratio
T	Temperature °C
V	Speed m/s
w	Water
W	Work Joule
x	Dryness fraction
X	Salinity.PPM
y	Independent variable response
Z	Height
0	Reference (dead) state
η	Efficiency
ψ	Specific flow exergy J/kg

the operating costs [13] as well as, requiring are least three main steps, precooling, crystallization, and separation [12] and [14].

Formation of ice crystals starts depending on many factors including the design of the used equipment and this leads to ice formation either as a frozen layer on the cooling surface or with the mother refrigerant itself [15]. Rane and Jabade [16]suggested a freeze concentration system (FCS) utilising a heat pump system and avoids the separation within the ice brine with a continuous cyclic melting-freezing process. The energy of the two stages compression system was expected to consume 9 to 11 kWh per meter cube water production with 8–12 cycle C.O.P [16].

A.A. Attia [17] suggested an auto reversed vapor compression heat pump system which avoids ice handling process in traditional freeze desalination systems. The ice washing process and melting progression

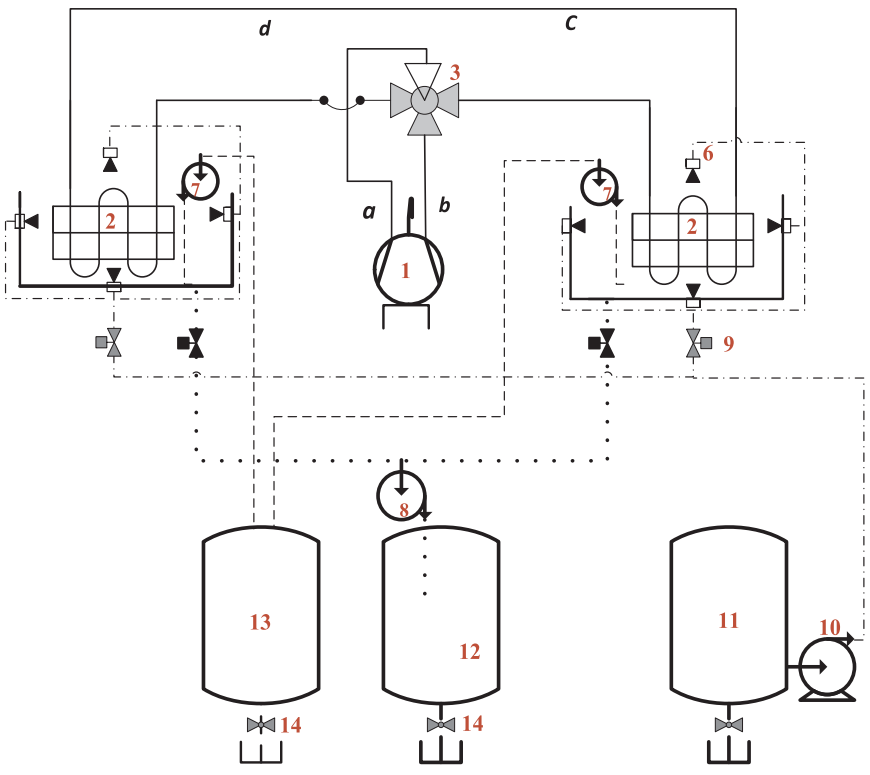

No	Item
1	Compressor
2	Heat Exchanger (Evaporator/Condenser)
3	Four Way (Reversible Valve)
4	Expansion Valve
5	Tank (Cooling/Heating)
6	Shower Jet (Nozzle)
7	Fresh water Pump
8	Brine Pump
9	Two-way Feed Valve
10	Feed Pump
11	Feed Tank
12	Brine Tank
13	Fresh water Tank
14	Drain Valve
15	Two Way Reject Valve

Fig. 1. Scheme diagram of the suggested freeze water desalination unit using reversed vapor compression refrigeration cycle.

were performed at the same place of ice creation. This was achieved by a special sequence of system operation. The thermal analysis of the system with simple cost analysis showed that the cost was lower than other desalination techniques for the same water production rate.

The first study reported in [17] aimed to present the idea and analysis of the basic thermal performance for different cycles not taking in considerations the effects of other operating parameters such as variation of freezing ratio, temperature and salt concentration. These parameters variations are critical to determine the working design parameters effects on the overall cycle performance. Hence it is the main motivation behind the current research. Besides that, developing exergy analysis for the cycle and comparing between the ideas of heat pump freeze desalination and other type of desalination techniques. .

This work aims to evaluate the operating parameters for a small-scale freeze desalination unit. A detailed study on the operating parameter with exergy analysis are introduced for a proposed actual unit working on a reversed vapor compression cycle that introduced by A.A. Attia [17]. Compressor capacity, ice ratio, supply water temperature, supply water salinity, and brine salinity will be investigated in this work. Thermal efficiency, cost efficiency and exergy efficiency are calculated and optimised according to the environmental regulation for brine salinity.

This study was built using the characteristics of freon R22 as a reference/maximum system performance as R22 is considered to be the most efficient freon, however it is not available for use due to its environmental aspects. Afterwards, the system was compared with R32 as a commercially available refrigerant with acceptable characteristics.

2. System sequence of operation

Fig. 1 shows the system schematic diagram consisting of two tanks, with two similar heat exchanger and vapor compression cycle. The vapour compression cycle consists of a compressor, an evaporator, a condenser, a four-way valve and an expansion valve. Each heat exchanger is operating as evaporator in a cycle and as a condenser in the following cycle. The operation begins by filling the right tank with the seawater supplied from the feed tank through the two-way valve to a certain level using the feed pump, then the compressor starts up. In this case, the heat exchanger inside the right tank is considered as evaporator while the heat exchanger in left tank is considered as the condenser for this phase of operation cycle.

After a definite cooling period –based on the selected ice ratio and the productivity– the saline water in right tank is converted to mixture of ice and brine solution. At this moment, the compressor shuts down and the brine water is rejected from the tank through a two-way valve to the brine tank leaving the ice block in the tank. The brine pump is used to accelerate its discharging.

The washing process starts by spraying a definite quantity of feed water using the nozzles system by opening a two-way valve and the feed water is supplied then to left tank. After completing this process, the cycle will be automatically reversed using the reversible valve -four-way valve- where the heat exchanger in right tank becomes a condenser where the ice block is melted to produce fresh water. In the same time, the other exchanger in the left tank works as an evaporator to produce a new block of ice. When the ice in right tank is completely melted, and the desalted (fresh) water temperature reaches the temperature of the supplied feed water the desalted (fresh) water is discharged using freshwater pump to the freshwater tank. If the ice block in the left tank is not completely formed with the required ice ratio the spraying using washing system starts to cool the condenser heat exchanger with sea water to keep COP of vapor compression cycle as much high as possible. These steps are repeated with the formed ice in the left tank.

3. System operating analysis

Fig. 2 represents the ln(P)-h diagram for the operating cycle with allocated critical points.

The coefficient of performance of the vapor compression cycle can be calculated using the below equation

$$C.O.P = \frac{cooling\ effect}{work\ input} = \frac{Q_L}{W} = \frac{h_a - h_d}{h_b - h_a} \quad (1)$$

The cooling effect is the summation of the sensible released heat from the salt water to reduce its temperature from T_{supply} to $T_{freezing}$ and the latent heat that was removed to convert water from its liquid phase to an ice solid phase. This cooling effect can be expressed as shown in equation (2).

$$Q_L = m \times (C_{P_{Supply}} T_{supply} - C_{P_{freezing}} T_{freezing}) + R \times m \times L.H.F \quad (2)$$

The freezing point of seawater with salinity percentage range (0.5–4) % was expressed as function in salinity in [18] as follow:

$$T_{freezing}(^{\circ}C) = -0.5369 \times S - 0.0172 \quad (3)$$

The supply seawater specific heat at different supply temperature was stated by [19] in equation (4).

$$C_{P_{freezing}} = 4186.8 \times \left(0.505 + 0.0018 T_{freezing} + 4.3115 \frac{S}{T^2_{Freezing}} - 0.0008 S + 0.00002 S T_{freezing}\right) \quad (4)$$

The latent heat of freezing can be calculated at different water salinity percentages within range (0.5% to 4.5%) and average freezing temperature of −2 °C using the following correlation [20]:

$$L.H.F = 4186.8 \times \left(79.68 - 0.505 T_{freezing} - 0.0273 S + 4.3115 \frac{S}{T_{freezing}} + 0.0008 S T_{freezing} - 0.0009 T^2_{freezing}\right) \quad (5)$$

Then, the compressor work was calculated using:

$$W = \frac{Q_L}{C.O.P}\,[\mathrm{kJ}] \quad (6)$$

The decrease in the C.O.P of the vapor compression cycle is only affected by the supply seawater temperature and there is no impact for the ice ratio on it. The C.O.P decreases with increasing the supply temperature that increases the required sensible heat removal [17]. So,

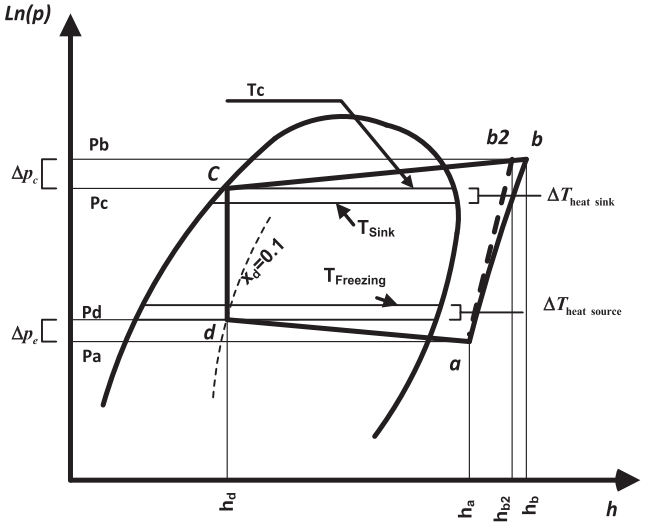

Fig. 2. Location of critical points on Ln (P)-h diagram.

the C.O.P values were taken according to the supply water temperature value as estimated in [17].

The energy consumption per unit mass production of fresh water can be calculated using the equation below:

$$E = \frac{W}{R \times m}\text{kJ/kg} \tag{7}$$

Water productivity was calculated as stated by [17] as follow:

$$waterproductivity = \frac{60 \times 60 \times compressorpower(kW)}{Energyconsumed\left(\frac{kJ}{kg}\right)freshwater}[\text{kg/hr}] \tag{8}$$

The brine solution can be predicted by making Mass and salinity balance as proposed in [21]and [22] as follow:

$$X_b = (X_f M_f - X_d M_d)/M_b \tag{9}$$

$$M_b = CR \times X_f \tag{10}$$

$$M_b = M_f - M_d = (1 - R) \times M_f \tag{11}$$

$$M_d = R \times M_f \tag{12}$$

Substituting in equation (11) leads to:

$$(1 - R) \times M_f \times X_b = M_f \times X_f - R \times M_f \times X_d \tag{13}$$

Then the icing ratio can be calculated by equation (14):

$$R = \frac{X_f(1 - CR)}{X_d - CRX_f} \tag{14}$$

The specific energy consumption per meter cube production of fresh water can be estimated by:

$$\text{specificenergyconsumption} = \frac{E(\text{kJ/kg}) \times 10000}{3600}, kW/m^3hr \tag{15}$$

4. Energy and exergy analysis

In the past, energy utilisation was calculated based on the first law of thermodynamics but recently the concept of exergy based on the second law of thermodynamics has been used to analyse these processes as it provides better insights when evaluating systems performance, efficiency of resources and environmental impacts in addition to the economic processes. [23]

Exergy analysis is the real application of the second law of thermodynamics and it gives a better indication from quality perspective rather than quantities. It is also a measure of the system sustainability level and it gives a clear illustration where is the energy lost in any system. For these reasons, the exergy analysis for the proposed system is a very important issue as it is mainly a heat transfer based system that involves lots of energy conversions and energy losses as well. Increasing attention is being given to energy conservation, and this has resulted in increasing use of the exergy analysis concept for thermal systems analysis and performance evaluation. This concept is widely recognized as a necessary tool to quantify the thermodynamic losses in a given system or process

The performance of the system was studied from the exergy perspective to examine its efficiency. Two different cases of reversible cycle condenser were analysed and called case B1 and case B2. Case B1 in which the low temperature of brine water was utilised by pumping it to a heat exchanger to cool the condenser. Case B2 was based on rejecting the brine water directly without benefiting from it. Exergy destruction was calculated for each component in the cycle and the cycle efficiency was obtained. The analysis was done based on the following assumptions:

- Steady state processes with negligible potential and kinetic effect.
- Neglect heat losses.
- Neglect tubing pressure drops between the components.
- Dead state was taken as the environmental conditions (with ambient temperature of T_o = 25 °C and pressure of Po = 1 bar).
- Neglect the heat transfer between the system and its surrounding.
- Constant density for saline water, salt and the fresh water.
- Full refrigerant condensation at the condenser exit and full evaporation at the evaporator exit.

4.1. Steady-state energy and exergy analysis

The steady state reversible heat pump was analysed based on mass, energy, and exergy balances. The mass conservation equation at each component can be expressed by:

$$\sum \dot{m}_i = \sum \dot{m}_o \tag{16}$$

4.2. Energy conservation

The energy conservation equation is:

$$E_i = E_o \tag{17}$$

The inlet and outlet energies of the system can be expressed by the net heat, work and mass transferred through the control volume as follow:

$$\dot{Q}_{cv} + \dot{m}_i\left(h_i + \frac{V_i}{2} + gZ_i\right) = \dot{W}_{cv} + \dot{m}_o\left(h_o + \frac{V_o}{2} + gZ_o\right) \tag{18}$$

4.3. Exergy balance

Exergy measures the energy ability to produce work and is equal to the optimum amount of work that can be produced from a fixed amount of energy. Therefore, the exergy of such systems relying on reversed heat engine operating on Carnot cycle is related to the heat transfer amount (Q), the fluid temperature (T) and the ambient temperature (T_o) and is given as:

$$Ex = \eta_{carnot} \times Q = \left(1 - \frac{T_o}{T}\right)Q \tag{19}$$

And as reported in [24] , at steady state conditions, the exergy balance is defined as the balance between the net exergy transmission by heat, work or mass flow through the control volume boundaries and the destructed exergy as shown in equation (20):

$$\sum \dot{m}_{in}\psi_{in} + \sum Ex_{Q_{in}} + \sum Ex_{W_{in}} = \sum \dot{m}_{out}\psi_{out} + \sum Ex_{Q_{out}} + \sum Ex_{W_{out}} + E_{xd} \tag{20}$$

Where:

$$\psi = (h - h_0) - T_0(S - S_0)J/kg \tag{21}$$

Due to exergy destruction inside the system or the process, the leaving exergy from the control system is always less than the entered exergy to the control volume. The rate of exergy destruction E_{xd} in the general exergy balance equation is directly proportional to the entropy generation rate [25]and is given by equation (22).

$$E_{xd} = T_0 S_{gen} \tag{22}$$

The total exergy destruction can be calculated by summation of the individual exergy destruction through each component of the system as follow:

$$\sum \dot{EXD}_i = \dot{EXD}_{comp} + \dot{EXD}_{exp} + \dot{EXD}_{ev} + \dot{EXD}_{cond,reversied} \tag{23}$$

The second low efficiency for the components (e.g., component i) can be written as

$$\eta_{\Pi,i} = \frac{EX_{out}}{EX_{in}} = 1 - \frac{EXD_i}{EX_{in}} \quad (24)$$

The second low efficiency for the entire desalination system can be written as

$$\eta_{\Pi,system} = \eta_{\Pi,comp} \times \eta_{cond-B} \times \eta_{exp} \times \eta_{ev} \quad (25)$$

Fig. 3 that represents energy balance for different system components.

From the description given above, the final exergy for individual components can be calculated based on their individual conditions as follow:

4.4. Compressor

$$h_a + w_c = h_2 \quad (26)$$

$$(h_a - h_0) - T_o(S_a - S_0) + w_c - ((h_b - h_0) - T_o(S_b - S_0)) = Exd_{comp} \quad (27)$$

4.5. Expansion valve

$$h_4 = h_5 \quad (28)$$

$$(h_c - h_d) - T_o(S_c - S_d) = Exd_{ex} \quad (29)$$

$$\therefore T_o(S_d - S_c) = Exd_{ex} \quad (30)$$

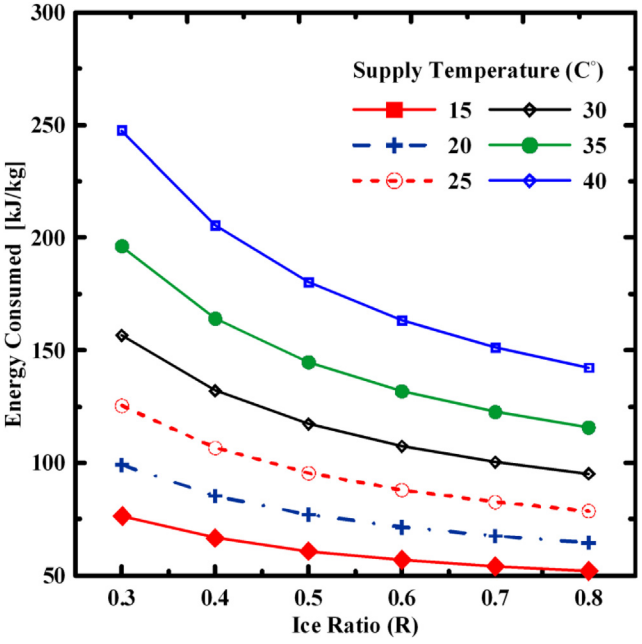

Fig. 4. Energy consumption at different supply temperature and ice ratio for salinity 35,000 PPM.

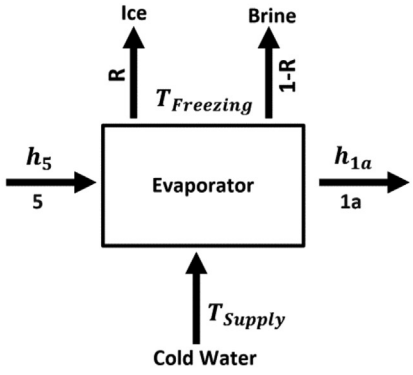

Evaporator.

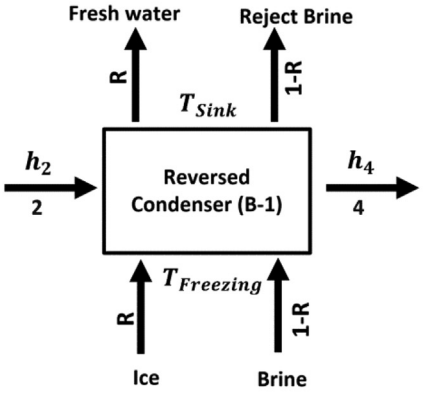

Condenser (reversed cycle) with brine (B-1)

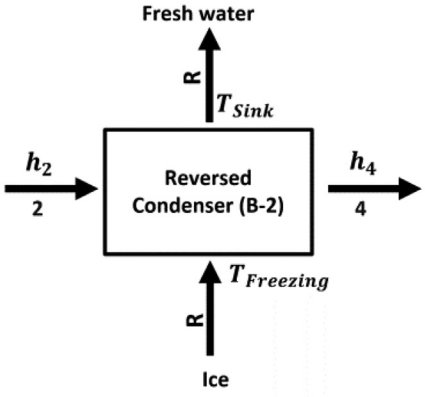

Condenser (reversed cycle) without brine (B-2)

Fig. 3. Energy balance for system different parts.

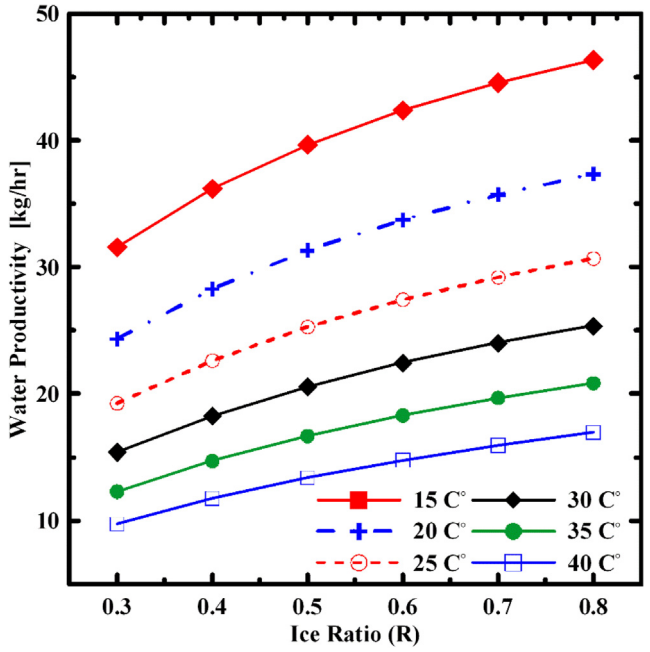

Fig. 5. Water productivity variation at different supply temperature, compressor power and ice ratio for 35,000 PPM salinity.

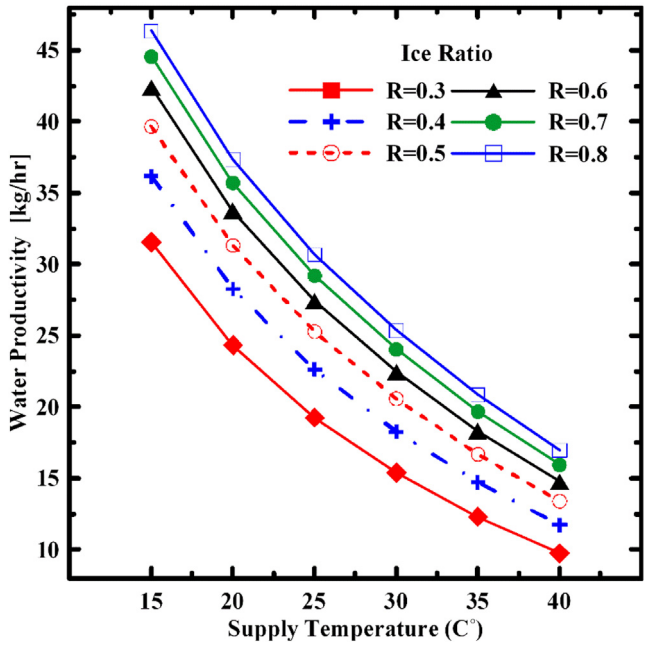

Fig. 6. Water productivity variation at different ice ratio, compressor power and supply temperature for salinity 35,000 PPM.

4.6. Evaporator (normal cycle)

$$m_w \times q_L + m_f \times h_5 = m_f \times h_{1a} \tag{31}$$

Where

$$q_L = R \times L.H.F + R \times C_{P_{Supply}} \times (T_{supply} - T_{freezing}) + (1 - R) \times C_{P_{brine}} \times (T_{supply} - T_{freezing}) \tag{32}$$

Water to refrigerant flow ratio:

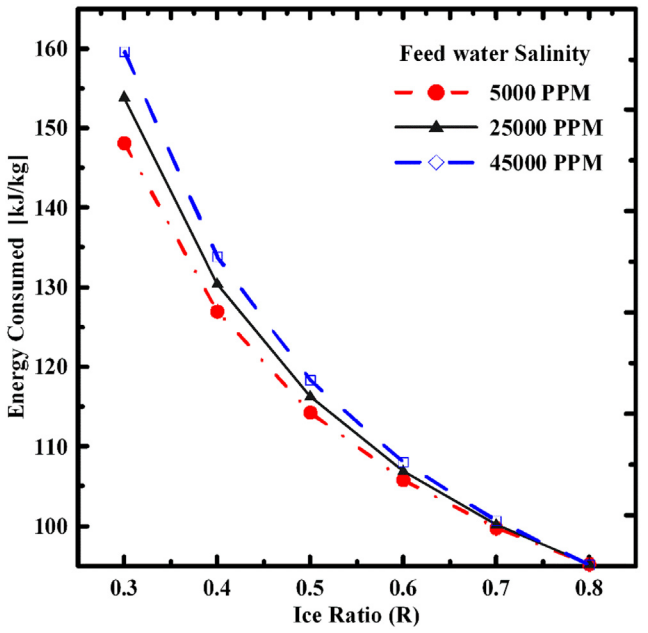

Fig. 7. Effect of feed water salinity variation on energy consumption at different ice ratio and supply water temperature of 30°C.

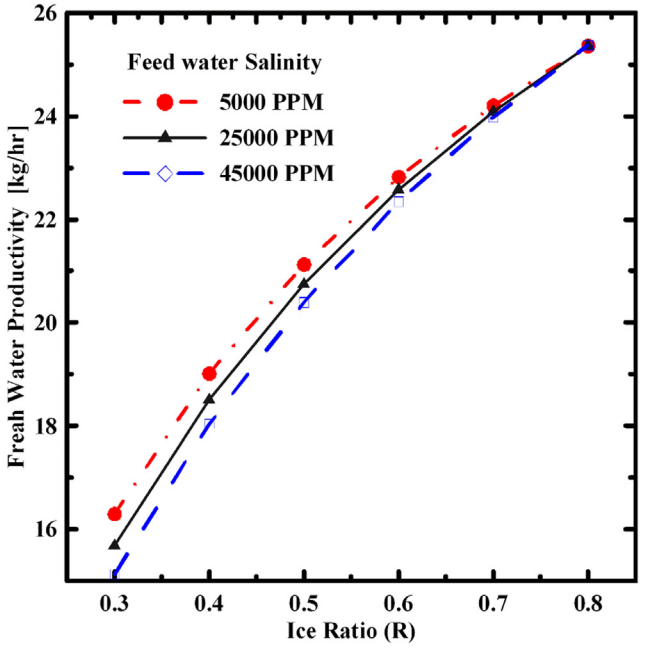

Fig. 8. Effect of feed water salinity variation on freshwater productivity at different ice ratio and supply water temperature at 30°C.

$$\frac{m_w}{m_f} = \frac{h_{1a} - h_5}{Q_L} \tag{33}$$

$$(h_d - h_a) - T_o(S_d - S_a) + R \times \frac{m_w}{m_f} \times \left(1 - \frac{T_o}{T_{freezing}}\right) \times LHF + R \times \frac{m_w}{m_f} \times \left[C_{P_{Supply}} \times (T_{supply} - T_{freezing}) - T_o \times C_{P_{Supply}} \times \ln\frac{T_{supply}}{T_{freezing}}\right] + R \times \frac{m_w}{m_f} \times \left[C_{P_{brine}} \times (T_{supply} - T_{freezing}) - T_o \times C_{P_{brine}} \times \ln\frac{T_{supply}}{T_{freezing}}\right] = Exd_{Ev} \tag{34}$$

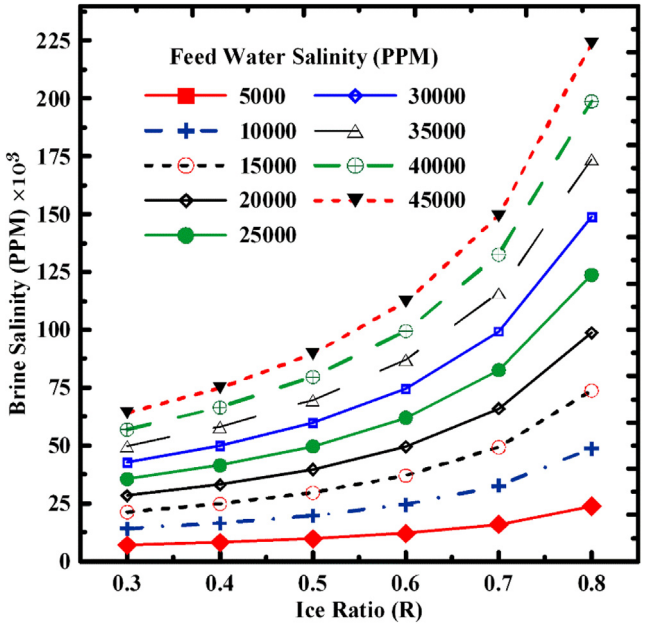

Fig. 9. Brine salinity variation with feed salinity at different ice ratios.

Table 1
Concentration ratio (CR) for different feed salinity (X_f) at different ice ratio(R).

X_f (ppm) /R	0.3	0.4	0.5	0.6	0.7	0.8
5000	1.39	1.6	1.9	2.35	3.1	4.6
10,000	1.4	1.63	1.95	2.43	3.22	4.8
15,000	1.41	1.64	1.97	2.45	3.26	4.87
20,000	1.42	1.65	1.98	2.46	3.28	4.9
25,000	1.42	1.65	1.98	2.47	3.29	4.92
30,000	1.42	1.66	1.98	2.475	3.29	4.93
35,000	1.42	1.66	1.99	2.48	3.3	4.94
40,000	1.42	1.66	1.99	2.48	3.3	4.95
45,000	1.42	1.66	1.99	2.48	3.31	4.96

Table 2
Optimal ice ratio (R) for different feed salinity (X_f) to keep the concertation ratio within range from 1.5 to 2.0.

X_f (ppm) / CR	1.5	1.6	1.7	1.8	1.9	2
5000	0.357	0.4	0.438	0.47	0.5	0.526
10,000	0.345	0.387	0.424	0.457	0.486	0.513
15,000	0.34	0.383	0.42	0.453	0.482	0.508
20,000	0.339	0.38	0.418	0.45	0.48	0.506
25,000	0.338	0.379	0.417	0.449	0.479	0.505
30,000	0.337	0.379	0.416	0.449	0.478	0.504
35,000	0.337	0.378	0.415	0.448	0.477	0.504
40,000	0.336	0.378	0.415	0.446	0.477	0.503
45,000	0.336	0.378	0.414	0.447	0.476	0.502

Table 3
Operating Parameter and their level in Taguchi analysis.

Parameter Description	Level 1	2	3	4	5
Supply temperature °C	15	25	30	35	40
Ice ratio	0.3	0.4	0.5	0.6	0.8
Salinity , PPM	5000	10,000	20,000	30,000	40,000

4.7. Condenser (reversed cycle) with brine (B-1):

$$m_f \times h_b = m_f \times h_c + m_w \times q_c \tag{35}$$

$$q_c = R \times L.\,H.\,F + R \times C_{P_{Supply}} \times (T_{sink} - T_{freezing}) + (1 - R) \times C_{P_{brine}} \times (T_{sink} - T_{freezing}) \tag{36}$$

Water to refrigerant flow ratio:

$$\frac{m_w}{m_f} = \frac{h_b - h_c}{q_c} \tag{37}$$

Exergy equation

$$(h_b - h_c) - T_o(S_b - S_c) + R \times \frac{m_w}{m_f} \times \left(1 - \frac{T_o}{T_{freezing}}\right) \times LHF + R \times \frac{m_w}{m_f} \times \left[C_{P_{fresh}} \times (T_{sink} - T_{freezing}) - T_o \times C_{P_{fresh}} \times \ln\frac{T_{sink}}{T_{freezing}}\right] + (1 - R) \times \frac{m_w}{m_f} \times \left[C_{P_{brine}} \times (T_{sink} - T_{freezing}) - T_o \times C_{P_{brine}} \times \ln\frac{T_{sink}}{T_{freezing}}\right] = EX_{condB-1} \tag{38}$$

4.8. Condenser (reversed cycle) without brine (B-2)

$$m_f \times h_2 = m_f \times h_4 + m_w \times q_c \tag{39}$$

$$q_c = R \times L.\,H.\,F + R \times C_{P_{Supply}} \times (T_{sink} - T_{freezing}) \tag{40}$$

Water to refrigerant flow ratio:

$$\frac{m_w}{m_f} = \frac{h_b - h_c}{q_c} \tag{41}$$

Exergy equation

$$(h_b - h_c) - T_o(S_b - S_c) + R \times \frac{m_w}{m_f} \times \left(1 - \frac{T_o}{T_{freezing}}\right) \times LHF + R \times \frac{m_w}{m_f} \times \left[C_{P_{fresh}} \times (T_{sink} - T_{freezing}) - T_o \times C_{P_{fresh}} \times \ln\frac{T_{sink}}{T_{freezing}}\right] = EX_{condB-2} \tag{42}$$

5. Results and discussion

5.1. Icing ratio and saltwater temperature effect

The effect of saltwater supply temperature on the energy consumption was studied in the range from 15°C to 40°C with 5 °C temperature step for ice ratios ranging from 0.3 to 0.8. Fig. 4 represents the energy consumption variation at different supply temperature.

It can be noted that the higher the percentage of ice ratio, the less energy is consumed. That's because as the percentage of ice ratio increases, the latent heat term increases while the sensible heat term remains constant. Thus, the whole quantity of heat released increases slightly with increasing the ice ratio. Despite this increase, the freshwater mass increases with ice ratio increase, but with a greater value than the heat removed and thus the energy consumption decreases with increasing ice ratio at all supply water temperature.

On the other hand, at any icing ratio, the supply water temperature has an obvious effect on the energy consumed as it increases the sensible heat required to reduce the supply water temperature up to the freezing point with the constant ice latent heat. Thus, the total amount of heat removed increases directly when increasing water temperature.

A small compressor of capacity 1 hp was selected to be studied to evaluate the unit productivity. The effect of supply temperature and ice ratio on the freshwater production is shown in Fig. 5.

For all saltwater supply temperatures, the freshwater productivity increases with the increase of ice ratio for the same illustration above.

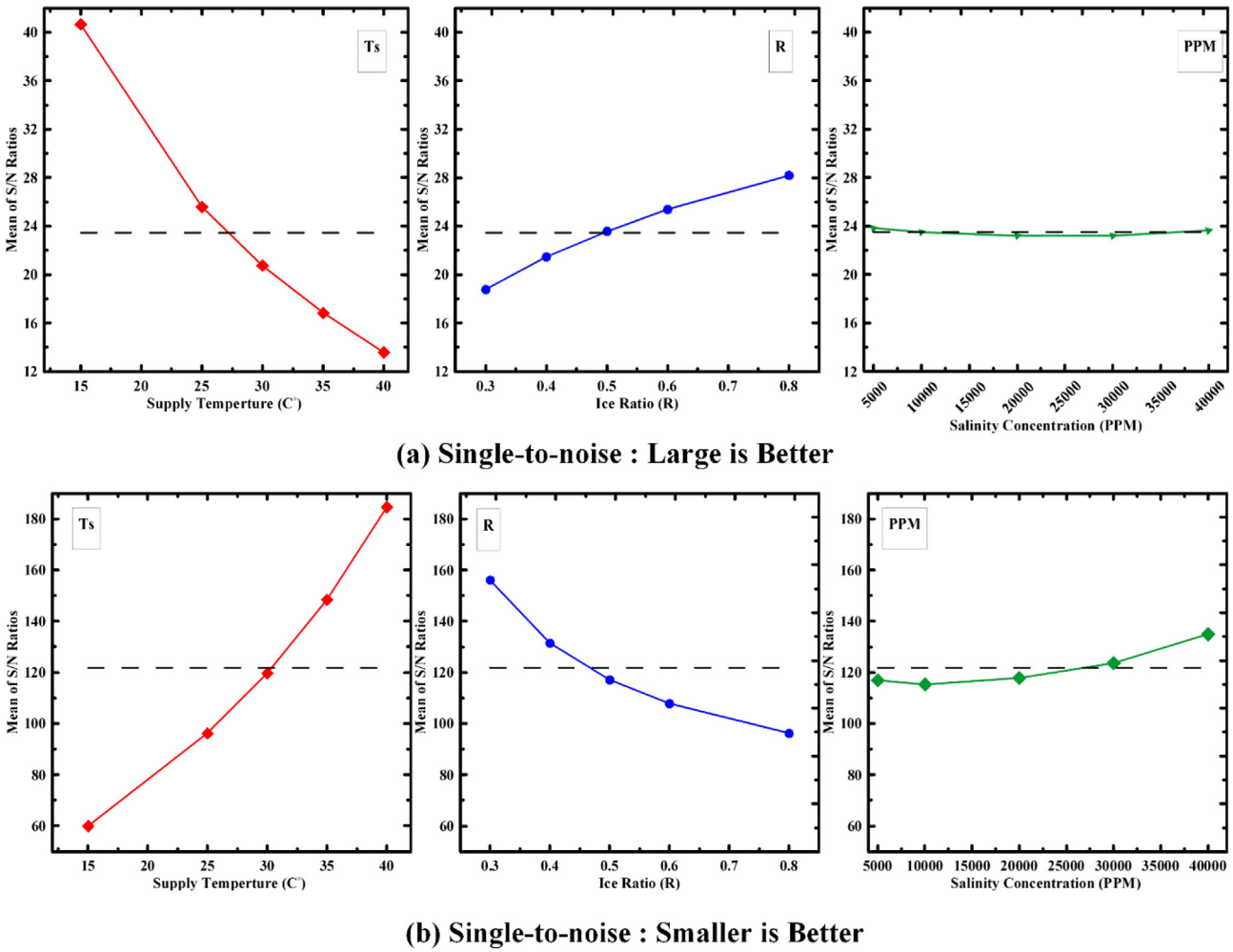

Fig. 10. Effects of each independent studied parameter on (a) fresh water productivity and (b) energy consumption.

Table 4
Exergy analysis for individual components of the reversed heat pump desalination system at R = 0.5, S = 3.5% and Ts = 25 °C.

ITEM	Exergy in (kJ/kg)	Exergy out (kJ/kg)	Exergy destruction (kJ/kg)	Exergy loss %	η_{2nd} %
Compressor	202.5	190.2	13.3	6.56	93.4%
Expansion valve	186.3	164.3	22	11.8	88.2%
Evaporator	127	80	47	37	63%
Reversed Condenser (B-1)	190	143	47	24.7	75.3%
Reversed Condenser (B-2)	190	131	59	31	69%

On the other hand, at any icing ratio the increase in water supply temperature decreases the water productivity due to the increase in the energy consumption as shown in Fig. 6.

5.2. Water salinity effect

The effect of salinity was studied in the range from 5000 to 45,000 ppm. The energy consumption showed a significant increase with salinity increase at the low icing ratio compared with the energy consumed at high salinity ratios as shown in Fig. 7.

The water productivity also decreases with salinity increase by a significant value at the low ice ratio while the decrease is not significant at higher icing ratios as shown in Fig. 8.

From Figs. 7 and 8 it can be concluded that, by increasing the water salinity from 5000 to 45000 ppm the energy consumption increases and the water productivity decreases by average value of 0.93% , 0.66% , 0.44% , 0.26% , 0.12% and 0.007% with ice ratio of 0.3 , 0.4 , 0.5 , 0.6 ,0.7 and 0.8 respectively.

5.3. Brine salinity effect

It is worth mentioning that desalination process is based on the removal of salts from the feed water and concentrate it in the rejected brine water which has to be discharged back to the environment. As reported in [15], the brine concentration must be no more than 2 times higher than the total dissolved solids concentration in order to avoid the negative effect on the aquatic environment. As discussed, energy consumption was decreasing, and productivity was increasing with the increase of ice ratio however, it must be limited and controlled according to the environment regulations.

Fig. 9 represents the variation of brine salinity with feed water salinity at different ice ratios. It shows that the when the ice ratio increases, the bine salinity increased up to 220000 ppm at ice ratio of 0.8 and feed salinity of 45000. This high concentration should be diluted in

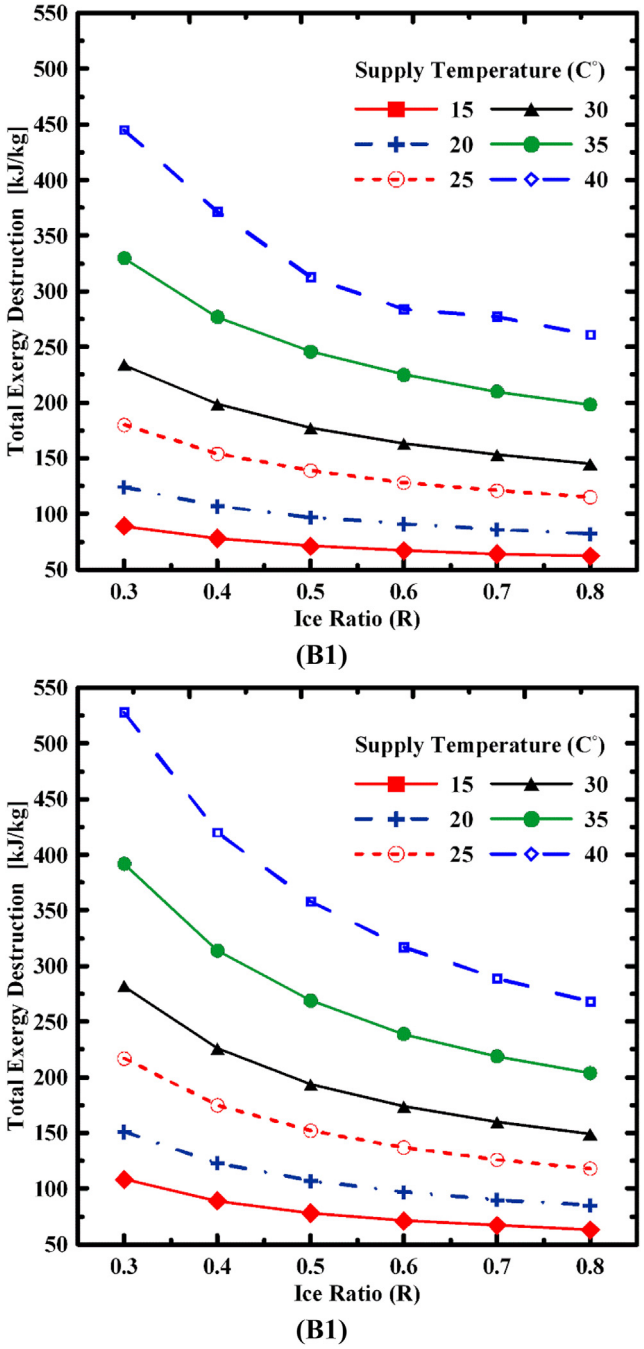

Fig. 11. The effect of icing ratios at different sea water temperature on total exergy destruction at 35,000 PPM salinity.

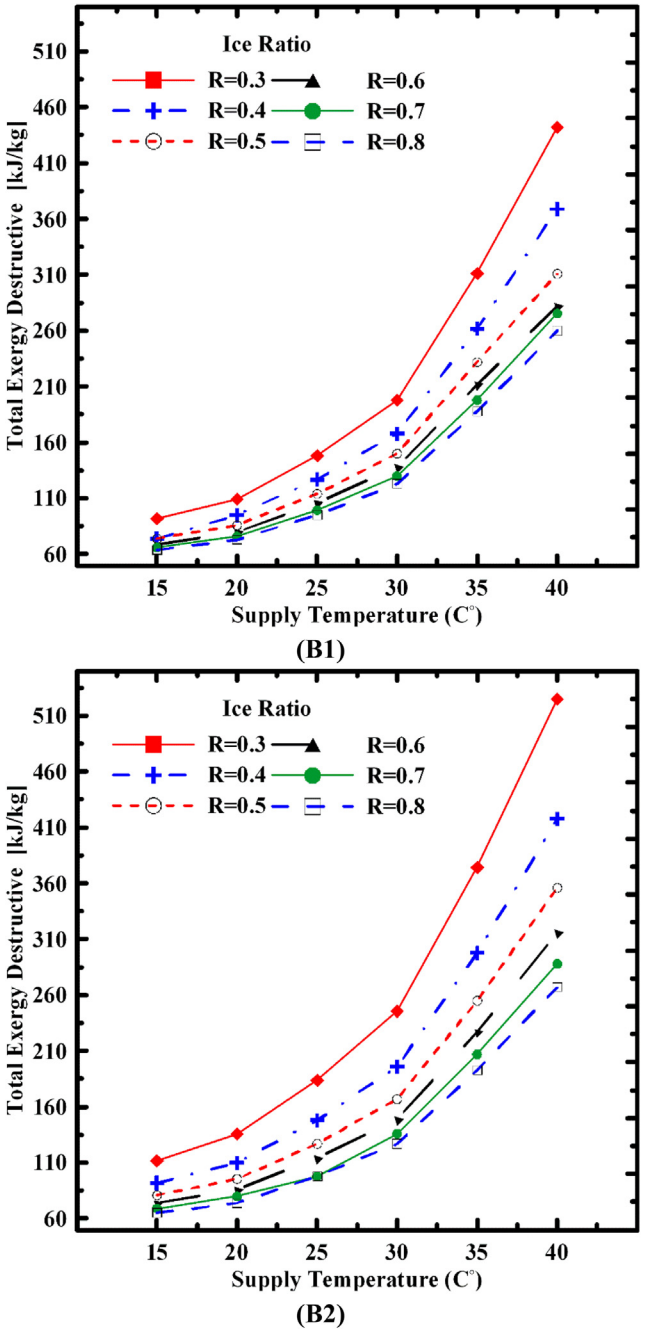

Fig. 12. The effect of seawater temperature on total exergy destruction at different ice ratios at 35,000 PPM salinity and compressor power of 1 HP.

order to avoid the bad impact on the environment.

Table 1 summarises the various concentration ratios of brine water with respect to feed water salinity. It is clear that, the concentration ratio increases from 1.38 to 4.6 with increasing the ice ratio from 0.3 to 0.8 for feed salinity of 5000. It is also increasing from 1.42 to 4.93 with the ice ratio increases from 0.3 to 0.8 for feed salinity of 45000.

The optimal ice ratio that is required to keep the brine concentration ratio is ranged within the environmentally friendly range - (1.5 – 2) according to [5]- can be calculated for distilled water salinity of 500 ppm and feed water salinity range from 5000 to 45000 ppm as summarised in table 2. The optimal ice ratio varied from 0.3 to 0.5 by increasing the concentration ratio from 1.5 to 2.

Desalination using high ice ratio of 0.8 gives higher productivity with the lowest energy consumption compared with other lower ice ratios but it produces high concentrated brine with concentration ratio and salinity up to 5 and 250000 ppm respectively. Therefore, the ice ratio higher than 0.5 cannot be used in conventional desalination methods where the high salt content in brine requires a specific disposal or treatment or causing other common problems like scaling, fouling, corrosion, and high energy consumption [22].Due to the high cost of brine concentrate disposal technologies with high energy consumption, freeze melt desalination is a promising because energy requirements can be much lower than using alternative technologies.

Different outputs from different parameters variation were used in Taguchi optimisation to determine the most influencing parameter on the system performance. This method is optimising different factors to give the optimum system performance. The performance was evaluated using both freshwater productivity and energy consumption as an

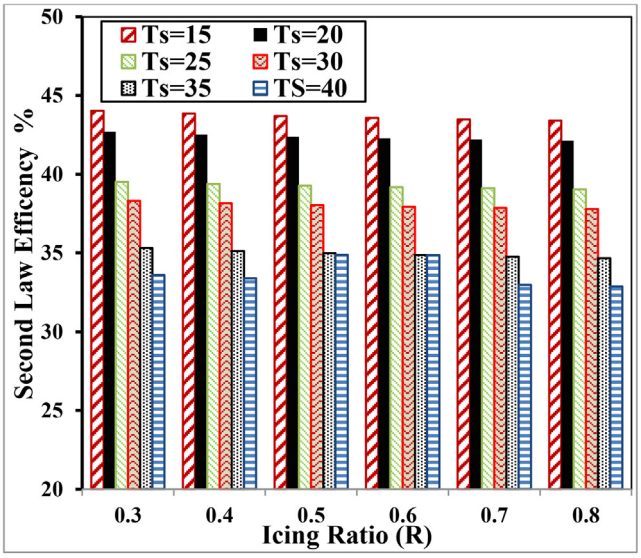

Fig. 13. Second law efficiency variation with supply temperature at different ice ratio for cycle with condenser (B1) and condenser (B2) with salinity 35,000 PPM .

index. Five levels of the independent parameter were considered as shown in Table 3.

The minimum number of trials can be determined as [26]:

$$N_T = 1 + N_P(N_L - 1) \tag{43}$$

Where $N_T$the minimum number of trials is, N_P is the number of parameters, and N_L is the number of levels of each parameter.

A standard L25 (3^5) Taguchi Orthogonal Array was chosen to design the experiments. The structure of array includes 25 combinations of the three independent parameters is shown in Table 2.

In the Taguchi method, the trial data can be analysed based on the signal to noise (S/N) ratio. For the present analysis The best level of each parameter can be indicated by selecting the levels with the largest fresh water productivity 'larger is better' which are defined using Eqn.44 and smallest energy consumption 'smaller is best' which are defined using Eqn.45 [27].

$$S/N = -10\log\left[\frac{1}{n}\sum_{i=1}^{n}\frac{1}{y_i^2}\right] \tag{44}$$

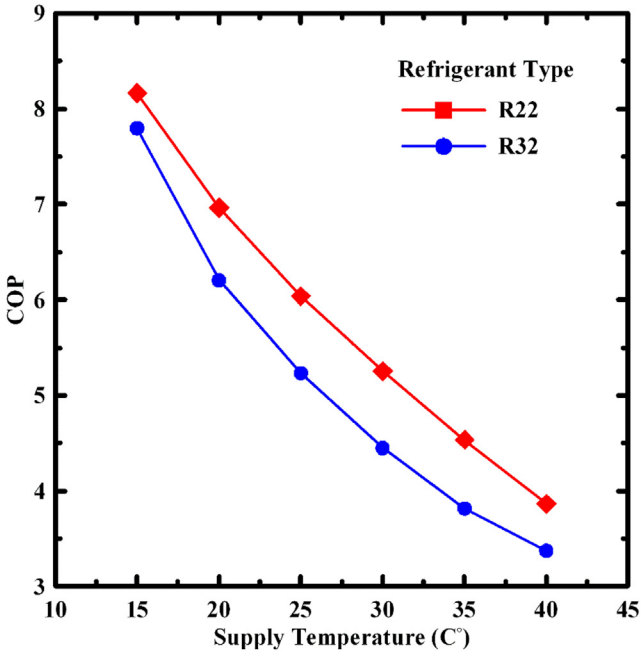

Fig. 14. A comparison of cycle COP using R 22 and R 32 at different supply temperatures.

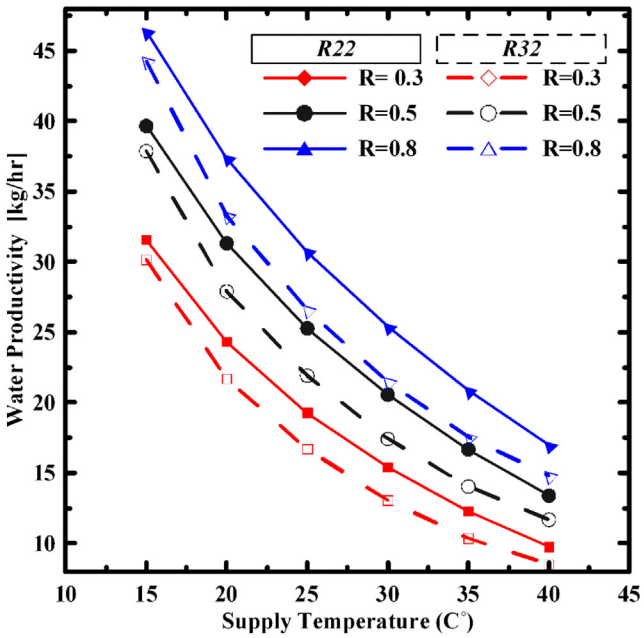

Fig. 15. A comparison of system water productivity [kg/hr] using R 22 and R 32 at different supply temperatures.

$$S/N = -10\log\left[\frac{1}{n}\sum_{i=1}^{n}y_i^2\right] \tag{45}$$

Where, y is the response and n is the total number of trials.

The effect of the independent parameter on (S/N) ratio for water productivity and energy consumption is illustrated in Fig. 10. The supply water temperature has the largest effect on both productivity and consumption, followed by the ice ratio, and then salinity concentration. Finally, it can be seen that the salinity concentration does not significantly affect this desalination technique and can be neglected.

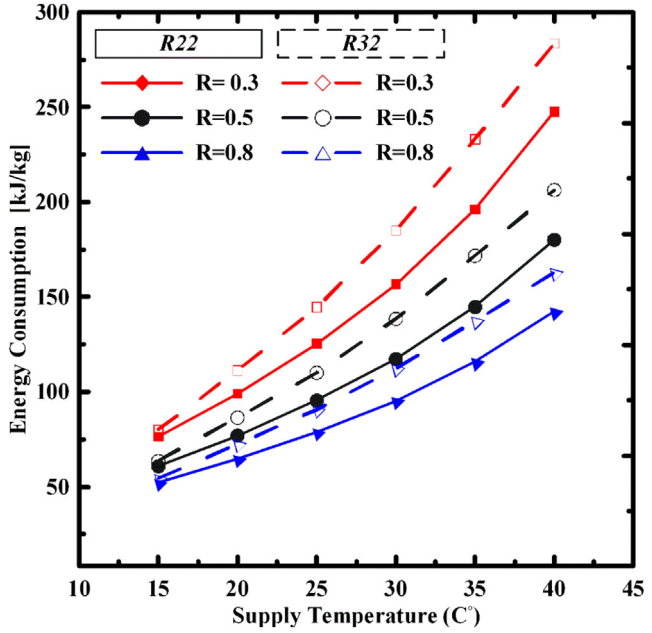

Fig. 16. A comparison of system energy consumption [kJ/kg] using R 22 and R 32 at different supply temperatures and 1Hp compressor.

5.4. Exergy analysis results

Exergy analysis results for the reversible heat pump desalination system at R = 0.5, S = 3.5% and T_s = 25 °C are listed in Table.4. Exergy destruction, Exergy loss percentage, and second law efficiencies are presented for the various system components.

From the table, it can be noted that, exergy losses in the compressor and the expansion valve are relatively small compared with other components. The compressor exergy losses recorded a value of 11 kJ/kg which is much less than the exergy losses in the evaporator of 32 kJ/kg and reversible condenser B2 34 kJ/kg. From this analysis, it can be concluded that the highest quantity of exergy losses occurs in the evaporator due to the special properties of R22 at the wet region (low entropy of the evaporator inlet S5). The exergy loss of condenser B1 (with brine low temperature utilisation) is lower than that of condenser B2 (without brine utilisation) which gives advantages of using condenser B1.

Fig. 11 shows the exergy destruction in the two cases of brine usage (B1) and (B2) versus icing ratios and Fig. 12 represents the exergy destruction at different saltwater temperature.

Results show that the more the icing ratio, the more reduction of the exergy destruction for all supply temperatures in both cases B1 and B2. The exergy destruction also increases with increasing seawater supply temperature and the more icing ratio increase. Also results showed that, the more icing ratios, the less the difference in exergy destruction between different supply temperatures. Fig. 13 shows the second law efficiency for the system versus icing ratio at different cases for different sea water inlet temperature.

Results show that, in case of B1 and at all supply temperatures, the change in icing ratio doesn't have a considerable effect on the second law efficiency however, the icing ratio critically affects the second system B2 and the efficiency was increasing by increasing the icing ratios. The current system proved to work with higher thermal efficiency than alternative desalination systems, such as reverse osmosis with membranes or flash systems. Thermal efficiency was about 44% at 25 °C supply water temperature with an icing ratio of 50% while the efficiency for osmosis membranes is about 30%.

This study was built based on R22 as a reference refrigerant due to its better performance and its thermal properties. For more realistic application and for currently available working fluids, system performance using R32 was estimated and compared with R22. Fig. 14 shows the difference between the heat pump performance when using R22 and R32 under different supply temperatures of salt water. From this figure, it can be seen that the coefficient of performance using R22 is higher than that COP using R32. the maximum increase in the COP of R22 compared to R32 was 18.8% at 35 °C.

The higher COP obtained using R22 was reflected as an increase in freshwater productivity at different salinity ratios as shown in Fig. 15. Fig. 16 shows a comparison between R22 and R32 at different supply temperatures. The system using R22 proved to have lower energy consumption compared with R32 system.

5.5. Proposed system cost comparison with other desalination systems

The cost to produce 1 kg of fresh water is estimated according to Equation (46) based on The world average price of 0.12 U.S per kW.h [28].

$$Cost = \frac{Price(\$/kWhr) \times CompressorPower(kW) \times 1000}{WaterProductivity(kg/hr)} / m^3 \quad (46)$$

Table 5 summarise the cost and energy estimation for water production using different desalination systems. From the table, it can be concluded that, the proposed system has lower energy consumption and production cost compared with humidification and dehumidification, membrane desalination and multi-effect desalination. It can also be noted that it has higher cost compared with totally developed techniques like reverse osmosis, but with more development of the proposed system, lower costs can be achieved in the near future.

6. Conclusion

Desalination by freezing is one of the promising desalination methods due to lower energy consumption. The effect of salinity increase was significant on both energy consumption which increased and productivity which significantly decreased especially in low icing ratios while this effect decreases at higher ice ratios. With increase of ice ratio from 0.3 to 0.4, 0.5, 0.6, 0.7 and 0.8, the fresh productivity increased by 17.5, 31.3, 42.5, 51.6 and 59. 4% respectively while the specific energy consumption (kw/m3.hr) was reduced by 14.9, 23.8, 29.8, 34 and 37.3% respectively. Although the ice ratio of 0.8 gives the highest productivity and required the lowest compressor work, it is not suitable for conventional desalination methods and need special brine treatment

Table 5
A comparison of the current system with different desalination systems.

Item	Desalination Types Multi-stage flash (MSF)	Reverse osmosis (RO)	Multi-effect distillation (MED)	Membrane Distillation	Humidification Dehumidification	Proposed system a. R = 0.8 & 15 °C
Total energy consumption (kWh/m3)	10–16 [29] 19.58 and 27.25 [6]	3–4 [29] 4–7 [30]	5.5–9 [29] 14.45–21.35 [6]	43 without Waste heat. 10.3 with waste heat.[31]	45.3 [32]	16
Water cost ($/m3)	*1.16Average* [33]	*0.66Average* [33]	*0.86 Average* [33]	N/A	Less than 5 [31]	1.9

technology for an environmentally friendly system. The optimum ice ratio is 0.3 to 0.5 to produce brine salinity of concentration ratio from 1.5 to 2. The proposed system works with an acceptable thermal efficiency compared to some of the other desalination methods such as Multi-stage flash or Multi-effect distillation systems however, it is currently in the developing stage. Thermal efficiency was about 44% when the saltwater temperature at the entry was 25 °C and the icing ratio is 50%

CRediT authorship contribution statement

M.A. Abd Elrahman: Conceptualization, Software. **Saber Abdo:** Formal analysis, Writing - original draft. **Eslam Hussein:** Data curation, Resources. **Ahmed A. Altohamy:** Writing - review & editing. **Ahmed A.A. Attia:** Project administration, Supervision.

Declaration of Competing Interest

The authors declare that they have no known competing financial interests or personal relationships that could have appeared to influence the work reported in this paper.

Acknowledgment

This research was supported by Benha University, Egypt and the University of Bristol. with a high contribution from “Combustion and Energy Technology Lab”, Shoubra Faculty of Engineering.

References

[1] I. Darawsheh, M.D. Islam, F. Banat, Experimental characterization of a solar powered MSF desalination process performance, Therm Sci Eng Prog 10 (2019) 154–162, https://doi.org/10.1016/j.tsep.2019.01.018.
[2] M. El Bastawesy, S. Gabr, I. Mohamed, Assessment of hydrological changes in the Nile River due to the construction of Renaissance Dam in Ethiopia, Egypt J Remote Sens Sp Sci 18 (2015) 65–75, https://doi.org/10.1016/j.ejrs.2014.11.001.
[3] A. Amirfakhraei, T. Zarei, J. Khorshidi, Performance improvement of adsorption desalination system by applying mass and heat recovery processes, Therm Sci Eng Prog 18 (2020) 100516, , https://doi.org/10.1016/j.tsep.2020.100516.
[4] W.Y. El-Nashar, A.H. Elyamany, Managing risks of the Grand Ethiopian Renaissance Dam on Egypt, Ain Shams Eng J 9 (2018) 2383–2388, https://doi.org/10.1016/j.asej.2017.06.004.
[5] N. Voutchkov, Overview of seawater concentrate disposal alternatives, Desalination 273 (2011) 205–219, https://doi.org/10.1016/j.desal.2010.10.018.
[6] A. Al-Karaghouli, L.L. Kazmerski, Energy consumption and water production cost of conventional and renewable-energy-powered desalination processes, Renew Sustain Energy Rev 24 (2013) 343–356, https://doi.org/10.1016/j.rser.2012.12.064.
[7] GWI I. Desalination Media Kit 2017-2018. n.d.
[8] B. Kalista, H. Shin, J. Cho, A. Jang, Current development and future prospect review of freeze desalination, Desalination 447 (2018) 167–181, https://doi.org/10.1016/j.desal.2018.09.009.
[9] A.R. Glasgow, G. Ross, Purification of substances by a process of freezing and fractional melting under equilibrium conditions, J Res Natl Bur Stand 1956 (57) (1934) 137, https://doi.org/10.6028/jres.057.017.
[10] P.M. Williams, M. Ahmad, B.S. Connolly, Freeze desalination: An assessment of an ice maker machine for desalting brines, Desalination 308 (2013) 219–224, https://doi.org/10.1016/j.desal.2012.07.037.
[11] H.M. Curran, Water desalination by indirect freezing, Desalination 7 (1970) 273–284, https://doi.org/10.1016/S0011-9164(00)80201-5.
[12] M.S. Rahman, M. Ahmed, X.D. Chen, Freezing-melting process and desalination: Review of present status and future prospects, Int J Nucl Desalin 2 (2007) 253–264, https://doi.org/10.1504/IJND.2007.013549.
[13] Kadi K El, I. Janajreh, Desalination by Freeze Crystallization: An Overview, Int J Therm Environ Eng 15 (2017) 103–110, https://doi.org/10.5383/ijtee.15.02.004.
[14] W. Cao, C. Beggs, I.M. Mujtaba, Theoretical approach of freeze seawater desalination on flake ice maker utilizing LNG cold energy, Desalination 355 (2014) 22–32, https://doi.org/10.1016/j.desal.2014.09.034.
[15] M.V. Rane, Y.S. Padiya, Heat pump operated freeze concentration system with tubular heat exchanger for seawater desalination, Energy Sustain Dev 15 (2011) 184–191, https://doi.org/10.1016/j.esd.2011.03.001.
[16] M.V. Rane, Jabade SK. Freeze concentration system. (2002), https://doi.org/10.1017/CBO9781107415324.004.
[17] A.A.A. Attia, New proposed system for freeze water desalination using auto reversed R-22 vapor compression heat pump, Desalination 254 (2010) 179–184, https://doi.org/10.1016/j.desal.2009.11.030.
[18] K.G. Nayar, M.H. Sharqawy, L.D. Banchik, J.H. Lienhard, Thermophysical properties of seawater: A review and new correlations that include pressure dependence, Desalination 390 (2016) 1–24, https://doi.org/10.1016/j.desal.2016.02.024.
[19] ONo N. Specific,, Heat and Heat of fusion of Sea Ice, Phys Snow Ice Proc 1 (1967) 599–610.
[20] N.H. Aly, A.K. El-Fiqi, Mechanical vapor compression desalination systems - A case study, Desalination 158 (2003) 143–150, https://doi.org/10.1016/S0011-9164(03)00444-2.
[21] M. Marcovecchioa, P. Aguirrea, N. Scennaa, S. Mussatia, Global optimal design of Mechanical Vapor Compression (MVC) desalination process. vol. 28, Elsevier B.V. (2010), https://doi.org/10.1016/S1570-7946(10)28211-1.
[22] R. Kaplan, D. Mamrosh, H.H. Salih, S.A. Dastgheib, Assessment of desalination technologies for treatment of a highly saline brine from a potential CO2 storage site, Desalination 404 (2017) 87–101, https://doi.org/10.1016/j.desal.2016.11.018.
[23] V.G. Gude, N. Nirmalakhandan, S. Deng, A. Maganti, Desalination at low temperatures: An exergy analysis, Desalin Water Treat 40 (2012) 272–281, https://doi.org/10.1080/19443994.2012.671262.
[24] M. Aliyu, A.B. AlQudaihi, S.A.M. Said, M.A. Habib, Energy, exergy and parametric analysis of a combined cycle power plant, Therm Sci Eng Prog 15 (2020) 100450, , https://doi.org/10.1016/j.tsep.2019.100450.
[25] M. Ameri, Eshaghi M. Syed, Exergy and thermal assessment of a Novel system utilizing flat plate collector with the application of nanofluid in porous media at a constant magnetic field, Therm Sci Eng Prog 8 (2018) 223–235, https://doi.org/10.1016/j.tsep.2018.08.004.
[26] I. Kotcioglu, M.N. Khalaji, A. Cansiz, Heat transfer analysis of a rectangular channel having tubular router in different winglet configurations with Taguchi method, Appl Therm Eng 132 (2018) 637–650, https://doi.org/10.1016/j.applthermaleng.2017.12.120.
[27] A. Balaram Naik, Reddy A. Chennakeshava, Optimization of tensile strength in TIG welding using the Taguchi method and analysis of variance (ANOVA), Therm Sci Eng Prog 8 (2018) 327–339, https://doi.org/10.1016/j.tsep.2018.08.005.
[28] www.globalpetrolprices.com. Electricity prices 2020. https://doi.org/10.1016/j.apenergy.2013.10.065.
[29] N. Ghaffour, T.M. Missimer, G.L. Amy, Technical review and evaluation of the economics of water desalination: Current and future challenges for better water supply sustainability, Desalination 309 (2013) 197–207, https://doi.org/10.1016/j.desal.2012.10.015.
[30] S. Miller, H. Shemer, R. Semiat, Energy and environmental issues in desalination, Desalination 366 (2015) 2–8, https://doi.org/10.1016/j.desal.2014.11.034.
[31] A. Subramani, J.G. Jacangelo, Emerging desalination technologies for water treatment: A critical review, Water Res 75 (2015) 164–187, https://doi.org/10.1016/j.watres.2015.02.032.
[32] M.S. Mahmoud, Enhancement of solar desalination by humidification-dehumidification technique, Desalin Water Treat 30 (2011) 310–318, https://doi.org/10.5004/dwt.2011.2212.
[33] P.M. Williams, M. Ahmad, B.S. Connolly, D.L. Oatley-Radcliffe, Technology for freeze concentration in the desalination industry, Desalination 356 (2015) 314–327, https://doi.org/10.1016/j.desal.2014.10.023.